Chemosphere 166 (2017) 521–527

Contents lists available at ScienceDirect

Chemosphere

journal homepage: www.elsevier.com/locate/chemosphere

Bacterial disinfection in a sunlight/visible-light-driven photocatalytic reactor by recyclable natural magnetic sphalerite

Xingxing Peng [a, b, 1], Tsz Wai Ng [b, 1], Guocheng Huang [b], Wanjun Wang [b], Taicheng An [c, **], Po Keung Wong [b, *]

[a] School of Environmental Science and Engineering, Sun Yat-sen University, Guangzhou 510275, China
[b] School of Life Sciences, The Chinese University of Hong Kong, Shatin, NT, Hong Kong SAR
[c] Institute of Environmental Health and Pollution Control, School of Environmental Science and Engineering, Guangdong University of Technology, Guangzhou 510006, China

HIGHLIGHTS

- Enhanced photocatalytic disinfection in a designed small-scale reactor.
- Recycling of natural magnetic sphalerite (NMS) by adding magnetic field.
- Excellent recycle usage of photocatalyst without any treatment.
- Good disinfection efficiency to various Gram-positive and Gram-negative bacteria.

GRAPHICAL ABSTRACT

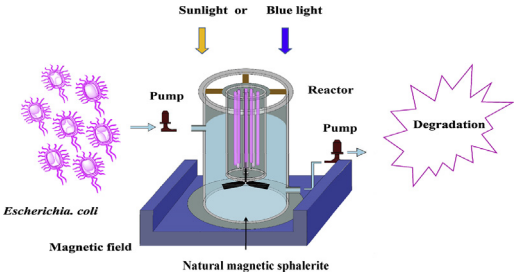

ARTICLE INFO

Article history:
Received 11 April 2016
Received in revised form
15 August 2016
Accepted 21 September 2016
Available online 5 October 2016

Handling Editor: Jun Huang

Keywords:
Natural magnetic sphalerite
Sunlight/visible-light
Bacterial disinfection
Disinfection reactor

ABSTRACT

A 5-L reactor was designed and used to enhance the sunlight/visible-light-driven (VLD) photocatalytic disinfection efficiency towards Gram-negative bacterium (*Escherichia coli*). Natural magnetic sphalerite (NMS) was used as the photocatalyst, which could be easily recycled by applying a magnetic field. Results showed that NMS with irradiation by the blue light emitting diode (LED) lamp could completely inactivate 1.5×10^5 cfu/mL of *E. coli* within 120 min in the first three runs. However, the inactivation efficiency of *E. coli* started to decrease in the 4th Run, while in the 5th run, the *E. coli* with the initial concentration of 5 logs was inactivated to 3.3 (blue-light) and 3.5 logs (sunlight), respectively. Moreover, the stability and deactivation mechanism of NMS during subsequent runs were also studied. The results showed that the decline of the photocatalytic activity was possibly attributed to adsorption of the bacterial decomposed compounds on the active sites. In addition, photocatalytic bactericidal mechanism of the NMS in the photocatalytic system was investigated by using multiple scavengers to remove the specific reactive species. Moreover, various Gram-positive bacteria including *Staphylococcus aureus*, *Microbacterium barkeri*, and *Bacillus subtilis* could also be efficiently inactivated in the photocatalytic system.

© 2016 Elsevier Ltd. All rights reserved.

1. Introduction

As an effective and sustainable method, photocatalysis has been intensively studied since the 1970s for water-borne pollutant

* Corresponding author.
** Corresponding author.
E-mail addresses: antc99@gdut.edu.cn (T. An), pkwong@cuhk.edu.hk (P.K. Wong).
[1] Equal contribution.

http://dx.doi.org/10.1016/j.chemosphere.2016.09.090
0045-6535/© 2016 Elsevier Ltd. All rights reserved.

degradation and fecal indicator bacteria (Choi and Hoffmann, 1995), especially the successful application of TiO_2 excited by UV irradiation (Li et al., 2008). However, compare to use of UV irradiation for photocatalytic pollutant degradation or microbial inactivation, use of visible light (VL) attract high research interests as 50% of sunlight composed of visible light. In addition, unlike expensive production of artificial synthetic material, naturally occurring semiconductor minerals are earth-abundant, part of which (such as rutile and sphalerite) have been successfully applied to heavy metal reduction, dyes degradation, and halohydrocarbons decomposition (Guo et al., 2012; Mignardi et al., 2012). Previous studies demonstrated that natural sphalerite (NS) and natural magnetic sphalerite (NMS) collected from mining sites in China could completely photocatalytically inactivate 7 logs of *E. coli* within 6 h using VL as light source in a laboratory-scale (50 mL) reactor (Chen et al., 2011; Xia et al., 2013).

The VL-induced heterogeneous reactions occurring at the NMS surface could result in generation of various reactive oxygen species (ROS) such as h^-, H_2O_2, and ·OH. These ROSs can effectively inactivate fecal inductor bacteria by oxidation (Brame et al., 2015). Previous works have revealed the photocatalytic disinfection using NMS as the photocatalyst in a 50 mL system. This method has been used to inactivate the fecal indicator bacteria (*Escherichia coli*) suspended in water in the designed reactor. Therefore, the development of a photocatalytic disinfection reactor using NMS as a cost-effective photocatalyst will be meaningful. Due to the high durability and corrosion resistance, non-toxic and earth-abundant nature of NMS, NMS is an excellent material for practical use in wastewater treatment.

In our previous studies, NMS were applied to conduct photocatalytic disinfection of *E. coli* under VL irradiation in a laboratory-scale reactor with a capacity of 50 mL (Chen et al., 2011; Xia et al., 2013). The goal of this study was to evaluate the efficiency of photocatalytic bacterial inactivation in a designed 5-L reactor using NMS as photocatalyst under different conditions (including night, cloudy day, or sunny day), which will be a foundation for further industrial application. The disinfection stability and deactivation mechanism during sequential disinfection cycles were investigated by X-ray diffraction (XRD), Fourier transform infrared spectroscopy (FT-IR), and Fluorescence excitation emission matrices (EEMs). The photocatalytic bactericidal mechanism was surveyed by adding different scavengers, as well as a comparison of photocatalytic inactivation of various microorganisms induced by NMS combined with VL irradiation.

2. Material and methods

2.1. Materials

The NMS, screening from a large number of NS samples, was collected from a lead-zinc mine in China mainland. The NMS powders were mechanically crushed, milled, and then passed through sieve pores with the sizes of <38 μm. All chemicals were of analytical grade (Sigma Co., USA), and all solutions were prepared using ultrapure water from a Millipore water purification system (Millipore Co., USA). All glasswares were washed using deionized water then sterilized in an autoclave (Hirayama HV-50, Japan) at 121 °C for 20 min.

2.2. Preparation of microorganisms and photocatalytic disinfection

Escherichia coli K-12, a representative Gram-negative bacterium, was used as model bacteria for the experiments, which was usually used as fecal bacteria indicator microorganism. 5-L suspension NMS and *E. coli* K-12 in the designed reactor (Fig. 1) was mixed by a plastic stirrer at a suitable speed. A blue light providing by blue light emitting diode (LED) lamp, which was a more suitable lightening source (Xia et al., 2015), was placed around and inside the reactor, as well as the intensity of the blue light was of 14 mW/cm^2 detected by a light meter (LI-COR, Lincoln, Nebraska, USA). *E. coli* K-12 was inoculated in the nutrient broth (Lab M, Lancashire, UK) at 37° C for 16 h in a shaking incubator. Ten mL nutrient broth mixture was collected in an Eppendorf tube at 13,000 rpm for 1 min. The harvested bacterial cells were washed twice with sterilized saline solution, and then re-suspended in sterilized saline solution. Appropriate volume of the collected bacterial cells was put into the 5-L reactor, to a final cell density of 1×10^5 cfu (colony forming unit)/mL. At different time intervals, aliquots of the samples were collected from the outlet by discarding the previous 20 mL. After serial dilution with sterilized saline solution, 0.1 mL diluted sample was spread on nutrient agar (Lab M, Lancashire, UK) plates then incubated at 37 °C for 24 h to determine the cell density by counting the survival colonies.

Similar to the inactivation of *E. coli* K-12, the inactivation of the three Gram-positive (*Staphylococcus aureus*, *Microbacterium barkeri* and *Bacillus subtilis*) bacteria was also assessed by a spread plate method with an extended incubation period of about 48 h at 37 °C. Suspensions of *B. subtilis* were prepared following the procedures by previous descriptions (Nakayama et al., 1996; Cho et al., 2004), which were incubated exceeding 50 h.

2.3. Characterization of photocatalysts

X-ray diffraction (XRD) pattern of NMS, surface chemistry properties as well as surface structure of the photocatalysts before use and at different cycles experiments were recorded using a DMAX-2400 (Rigaku, Japan, Cu Kα, λ = 0.15406 nm) with a secondary graphite crystal monochromator. The identification of organic compounds (including protein etc.) on the NMS surface was conducted using a FT-IR spectrometer (FTS-4000 Varian Excalibur Series) with attenuated total reflection (ATR) (Varian, Palo Alto, CA). Bands in the spectral region of 4000 to 800 cm^{-1} monitored with a resolution of 4 cm^{-1}, as well as each spectra was automatically corrected with an average of 256 scans. Samples were prepared as follows: the suspensions in different 5 cycles were evaporated by a freeze-drying technique, then the dry remaining was mixed with KBr to form pellets for FT-IR measurement (Elzinga et al., 2012; Kiwi and Nadtochenko, 2005).

2.4. Spectroscopic measurements

Fluorescence excitation emission matrices (EEMs) were measured on a F-7000 fluorescence spectrophotometer (Hitachi Co., Japan) with the scanning emission (Em) spectra from 290 to 500 nm obtained in 5 nm increments by varying the excitation (Ex) wavelength from 200 to 400 nm in 5 nm increments with a scan rate of 12,000 nm/min.

3. Results and discussion

3.1. Photocatalytic disinfection in different cycles under sunlight/visible light

Under visible light irradiation, the photocatalytic inactivation efficiency of *E. coli* K-12 in the large volume (5-L) reactor was same as that in the small volume (50 mL) reactor (Xia et al., 2013). To investigate the stability and reusability of the screened NMS, bacterial inactivation by NMS was conducted for five repeated cycles. The results of photocatalytic inactivation *E. coli* K-12 was effectively inactivated in different repeated cycles (Fig. 2), which were

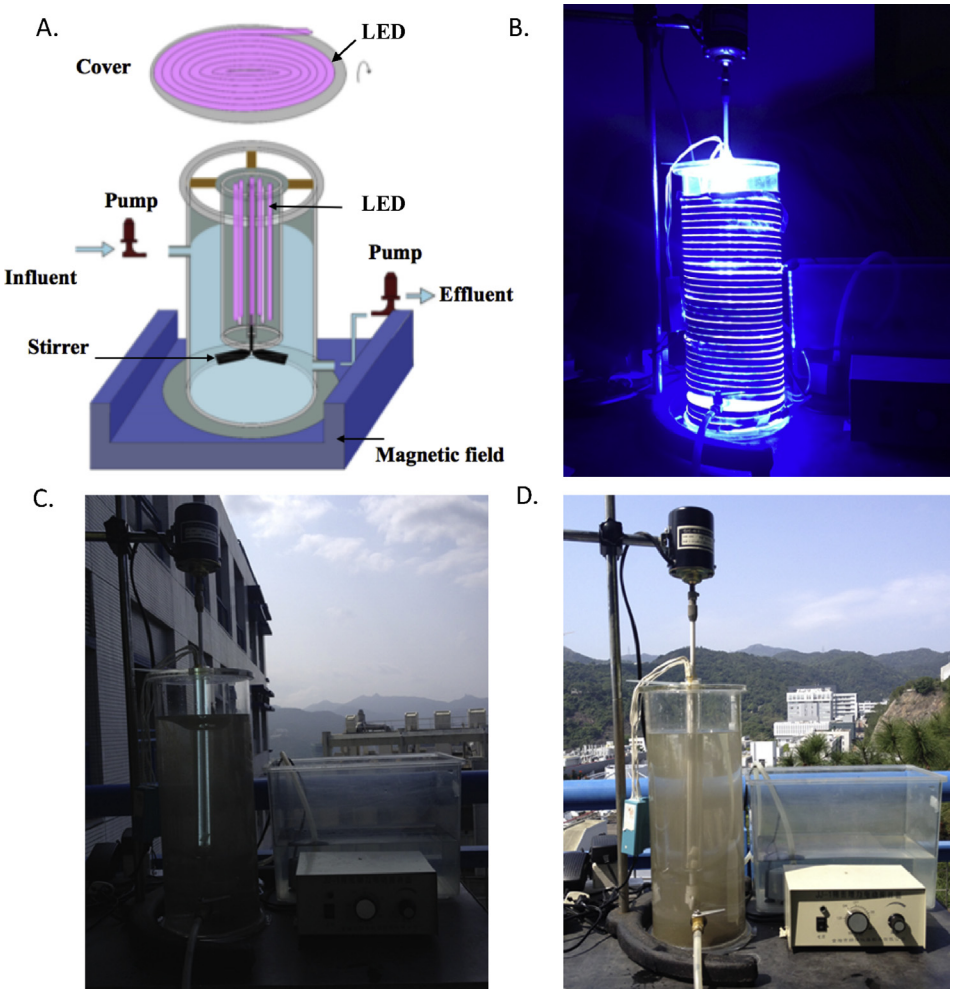

Fig. 1. (A) Diagrammatic drawing and (B-D) photo of photocatalytic NMS disinfection reactor for photocatalytic inactivation of bacteria (B) at night, and (C) in cloudy and (D) sunny days.

consistent with previous findings about bacterial inactivation or contaminants removal catalyzed by another photocatalysts (Ng et al., 2016; Yu et al., 2016). The bacterial inactivation efficiency was influenced by the intensity of visible light or UV (Fig. 1A–E). For example, fast inactivation was observed in 3rd cycle in which the light intensity was highest among different cycles. Temperature in different repeat cycles did not show good relationship with the bacterial inactivation. This result suggests that the temperature in a range of 20–30 °C does not affect the bacterial inactivation efficiency.

NMS is able to inactivate bacterial cells in five repeated cycles under blue light irradiation. The disinfection efficiency is slightly lower than that under sunlight irradiation (Fig. 2A–B). It is mainly due to the lower light intensity provided by the artificial light source. On the other hands, the disinfection efficiency is more stable as the intensity of light source is controlled. The slower inactivation in the 5th cycles is attributed to the accumulation of organic matters on the surface of NMS, which may also be caused by the residual cell debris on the surface of NMS. This passivation on catalysts surface also was found in other treatment systems (Gamalski et al., 2015; Xin et al., 2016).

In the 1st to 3rd cycles, there are strong correlations between bacterial photocatalytic inactivation efficiency and the intensity of UV (purple) or the VL (red) using the Pearson correlation analysis (Fig. 2E). It means that the stronger intensity of UV and VL, the better results of the NMS photocatalytic inactivation efficiency. However, in the 4th and 5th cycles, the correlation was weaker. Based on the batch experiments, the decrease in bacterial inactivation of NMS may be caused by the organic compounds on the surface of the NMS which decreased the contact areas (Xia et al., 2013; Yang et al., 2015).

3.2. Stability and reusability during cycle experiments

The stability and reusability of the NMS used as photocatalysts was investigated by 5 repeated cycles of *E. coli* inactivation experiments using recycled NMS without any treatment. The *E. coli* (10^5 cfu/mL^{-1}) in the photocatalytic system could be completely inactivated within 120 min under the VL irradiation using NMS as photocatalyst. However, the photocatalytic inactivation activities were decreased in the recycling experiments. Therefore, it will be very necessary to investigate deactivation mechanism to extend the lifetime of photocatalyst or avoid the rapid decrease of the *E. coli* inactivation, which was consistent with our previous study (Xia et al., 2013).

The deactivation mechanism was studied by the characteristics of surface properties of photocatalyst before and after being used in different cycles. According to X-ray diffraction pattern (XRD) analysis (Fig. 3A), as compared with JCPDS No.05-0566 data, the three strongest characteristic diffraction peaks (28.4°, 47.3° and

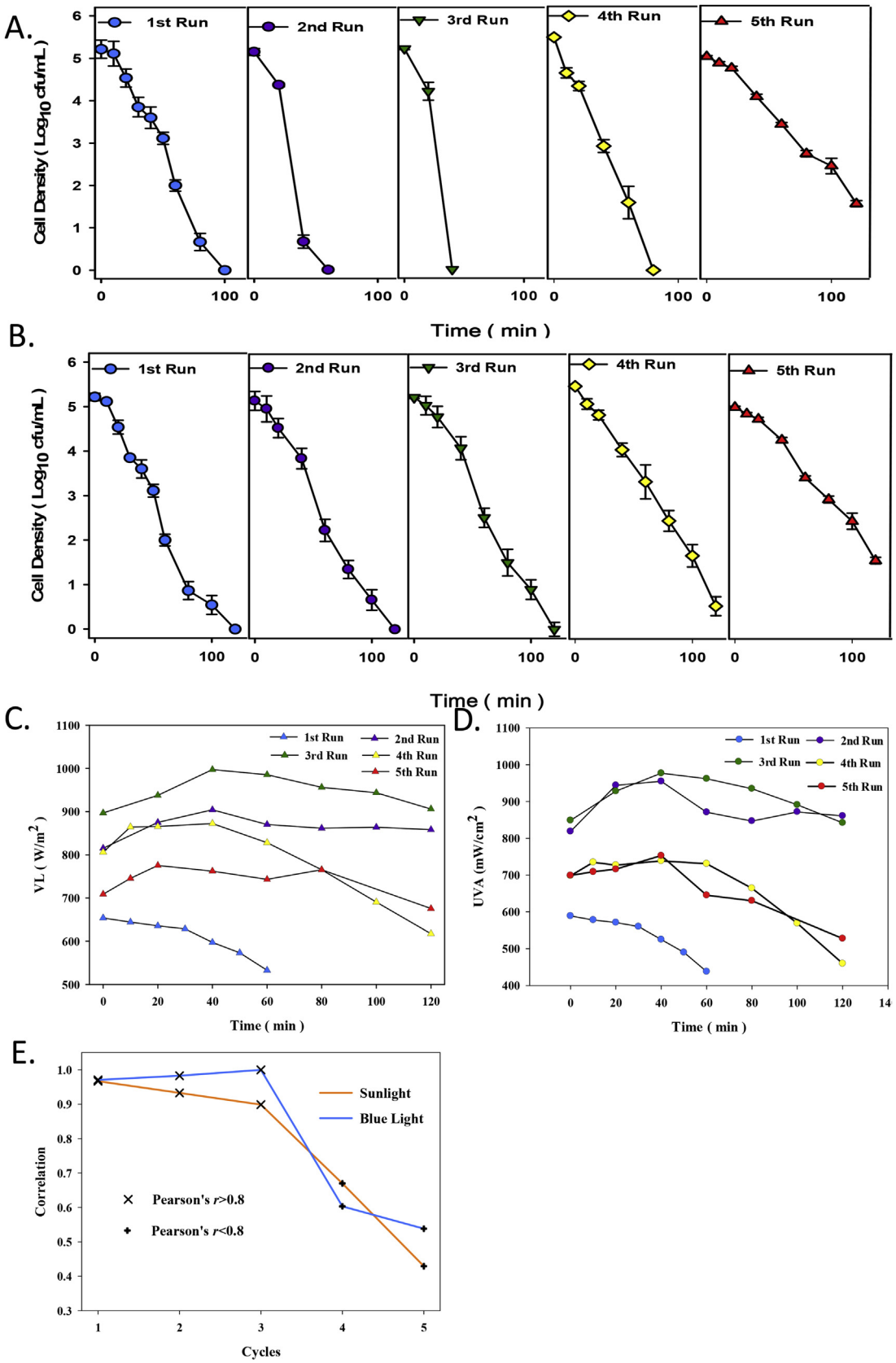

Fig. 2. The inactivation efficiencies of *E. coli* K-12 (10^5 cfu/mL, 5 L) by recycled NMS under (A) blue light irradiation (light intensity = 14.8 mW/cm^2) and (B) sunlight with the detected (C) VL and (D) UVA. (E) Correlation of bacterial photocatalytic inactivation between the UV (Purple) and the VL (Red) using the Pearson correlation analysis. Pearson's r was used to measure the relationship, where 1 is total positive correlation, 0 is no correlation. The Pearson's r > 0.8 means perfect relationship; Pearson's r < 0.8 means relatively worse relationship. (For interpretation of the references to colour in this figure legend, the reader is referred to the web version of this article.)

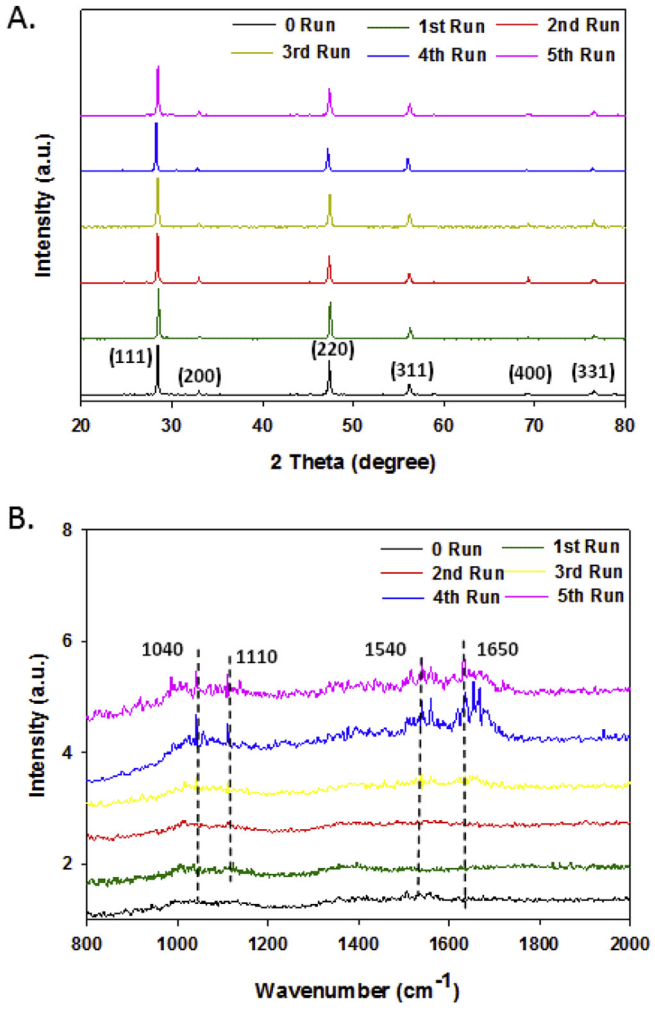

Fig. 3. Analyses of NMS sample collected at different cycle of visible light photocatalytic inactivation. (A) XRD spectra and (B) FT-IR spectra with bands in the spectral region of 800–2000 cm^{-1}.

56.1° correspond to (111), (220) and (311) planes, respectively) were characterized as a pure phase of cubic sphalerite. As for NMS, the intensity of the above three strongest diffraction peaks in XRD pattern was not obviously changed before use for five repeated cycles. Therefore, it can be confirmed that there is no obvious difference in main phase structure and surface properties of NMS before and after being used for five repeated cycles. However, during the multi-run recycling experiments of 4th and 5th Run, the photocatalytic disinfection activity was obviously decreased. Theoretically, if the drop of photocatalytic disinfection activity is due to photo-corrosion, an apparent change of the surface properties of the photocatalysts should be observed. This contradict to the results of XRD analysis. Therefore, further study on the surface properties of photocatalysts before use and in the later 5 cycle experiments was conducted by FT-IR analysis (Fig. 3B). Total 6 different absorption peaks (i.e., 1040, 1110, 1540, and 1650 cm^{-1}, respectively) on the surface of NMS showed slight or obvious changes before use and in the later 5 cycle experiments. The characteristic peaks at 1040 and 1110 cm^{-1} were a group of bands arising due to C=C stretching vibrations (Bhatt and Gohil, 2013), while the bands around 1540 and 1650 were attributed to COO^- symmetric stretching ($\nu_{coo\text{-}s}$) and C=O stretching of amide, quinone, or H-bonded conjugated ketones ($\nu_{c=o}$), respectively (Chen et al., 2014). The S=O (SO_2) band (2330 and 2360 cm^{-1}) was also observed (Duan et al., 2011). After 3 cycle of experiments, the peak intensity of C=C bands (1040 and 1110 cm^{-1}) were observed, while N=O bands (1540 and 1650 cm^{-1}) were significantly increased. Therefore, the *E. coli* in the photocatalytic system were not only inactivated but also severely distorted, ruptured, and even transformed into large biomolecules and organic debris, which may block photocatalytic active sites leading to the decrease of photocatalytic disinfection. This result was consistent with our previous lab-scale studies (Xia et al., 2013).

3.3. EEM analysis on the NMS reusability influenced by DOM

The technology of fluorescence quenching generally provides a specific bonding of quencher to fluorophores (Yamashita and Jaffé, 2008). The results of EEM spectra of dissolved organic materials (DOM) released from the severely distorted and greatly ruptured bacteria by the photocatalytic destruction were showed in Fig. 4. Three peaks with Ex/Em centered at 270/350 (F1), 220/350 (F2), and 350/410 nm (F3) were identified, which were attributed to protein-like compounds, and phenolic-like fluorophores, respectively. With an increase of re-cycles experiments, the fluorescence intensities of F1 and F2 sharply increased in the previous three runs then slightly decreased in the latter two runs. However, the same tendency of fluorescence intensities of F3 was investigated but very limited amount was found in the 5-L photocatalytic system compared to F1 and F2. The EEM results indicate that the bonding associated with the detected fluorophores was associated with the deactivation during the recycle experiments by blocking the activation sites, which was consistent with the results of XRD and FI-TR analysis (see Fig. 5).

3.4. Photocatalytic disinfection mechanism

Photocatalysis is known to produce a series of reactive species (RSs, including •OH, H_2O_2, $\bullet O_2^-$, h^+, and e^-) from e^--h^+ pairs, which are potentially involved in the bacterial disinfection (Wang et al., 2012). Considering multiple RSs in various photocatalytic systems may play quite different roles (Cho et al., 2004), different scavengers were used to remove specific RSs to determine the effects on the photocatalytic inactivation process. As the addition of all scavengers did not show toxicity to *E. coli* K-12 in 6 h treatment (Chen et al., 2011), the reduction in photocatalytic inactivation efficiency was mainly due to the removal of RSs by the corresponding scavengers. Various scavengers with proper dose quenched different RSs in the NMS photocatalytic system, including sodium oxalate (0.5 mM/L) for h^+, isopropanol (0.5 mM/L) for •OH, Cr(VI) (0.05 mM/L) for e^-, TEMPOL (2 mM/L) for $\bullet O_2^-$, and Fe(II)-EDTA (0.1 mM/L) for H_2O_2 (Cho et al., 2011). Without the addition of scavengers, the E. *coli* was almost completely inactivated within 2 h. Addition of excess isopropanol (0.5 mM/L) did not obviously affect *E. coli* K-12 disinfection, revealing a negligible role of •OH in bacterial disinfection. In the presence of excess sodium oxalate (0.5 mM/L), the level of bacteria was slightly higher than on scavenger and •OH scavenger, indicating that h^+ was not strongly involved in the photocatalytic disinfection process. The excess TEMPOL (2 mM/L) was used to effectively quench $\bullet O_2^-$, nearly inhibited the bacterial disinfection. However, the bacterial disinfection was partially inhibited by addition of excess Fe(II)-EDTA (remove H_2O_2) and Cr(VI) (remove e^-) with the disinfection efficiencies of 24.8 and 40.7% after 120 min treatment, respectively. The importance of RSs in the photocatalytic disinfection system follows the sequences of $\bullet O_2^- > H_2O_2 > e^- > h^+ >$ •OH. Thus it can be seen that the RSs of $\bullet O_2^-$ and H_2O_2 play critical roles during the photocatalytic disinfection process, which were consistent with previous study (Xia et al., 2013).

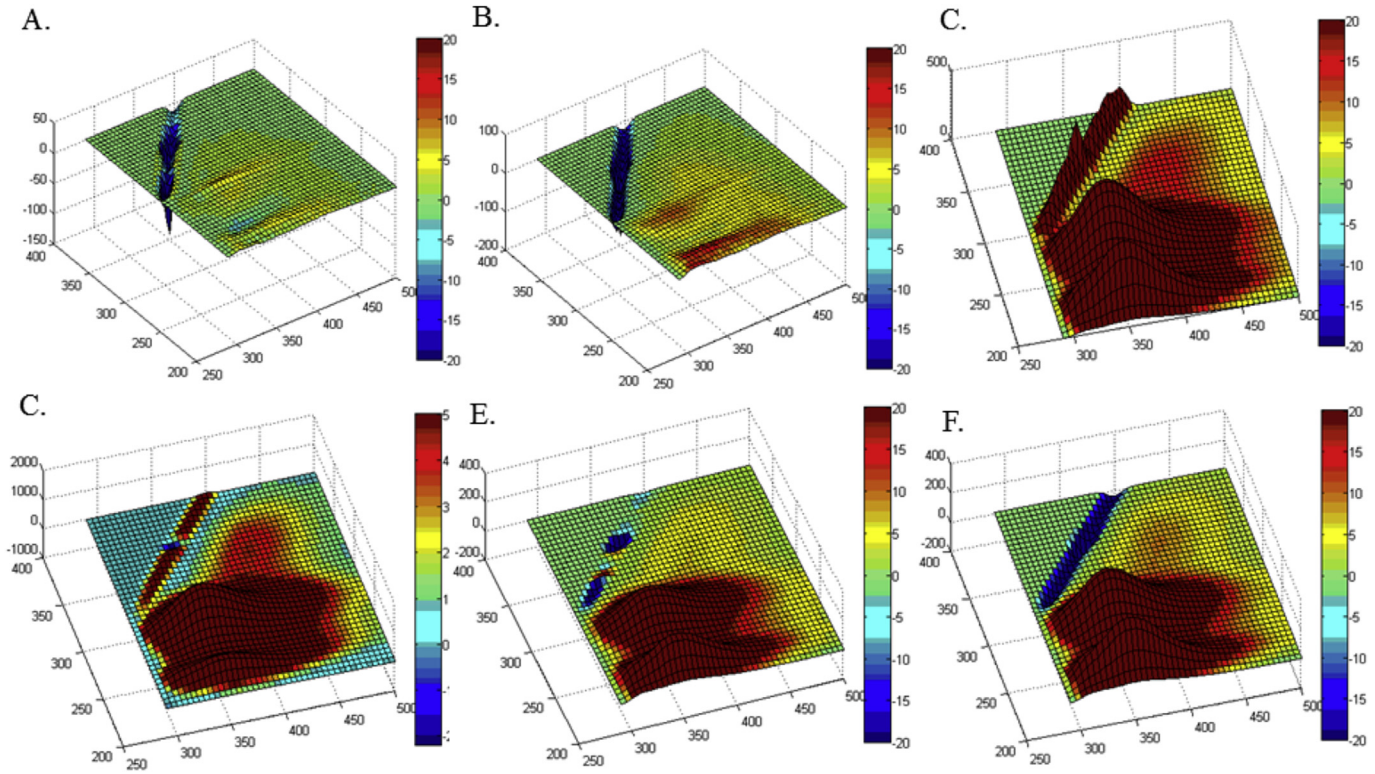

Fig. 4. EEMs of the control and 1–5 cycle experiments.

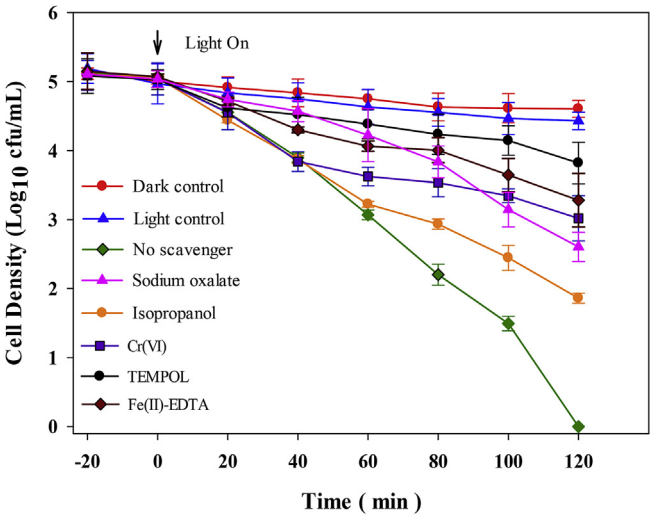

Fig. 5. Disinfection efficiencies using various chemical scavengers.

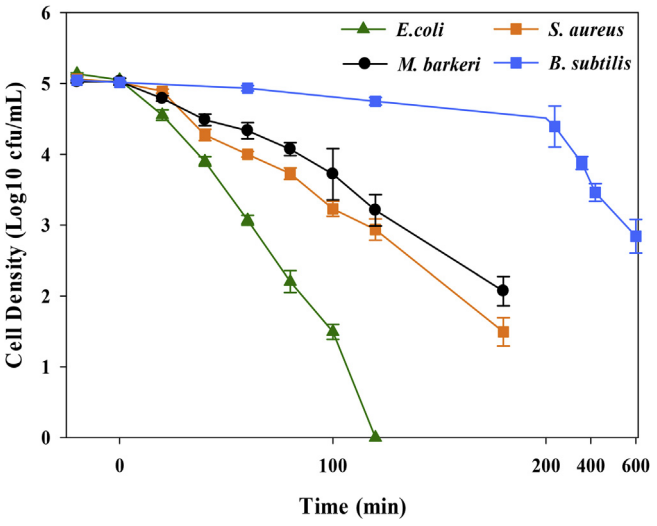

Fig. 6. Effect of the photocatalytic NMS reactor on disinfection of various bacteria: *Escherichia coli*, *Staphylococcus aureus*, *Microbacterium barkeri* and *Bacillus subtilis*.

3.5. Photocatalytic inactivation of various bacteria

The photocatalytic disinfection kinetics of various bacteria in the designed 5-L reactor was conducted under blue light. Generally, the five selected representative bacteria exhibited good photocatalytic inactivation in different extend (Fig. 6). Because of the thicker cell wall, the selected Gram-positive bacteria (*B. subtilis, S. aureus* and *M. barkeri*) showed higher resistant to the photocatalytic inactivation than the Gram-negative bacterium (*E. coli*). This result was consistent with the previous studies (Chen et al., 2013; Rodríguez-Chueca et al., 2015). As reported previously, *M. barkeri* was more resistant than *E. coli* but less than *B. subtilis* spore (Wiebke et al., 2012), as well as photocatalytic disinfection to the four selected bacteria was in the order of *E. coli* > *S. aureus* > *M. barkeri* > *B. subtilis*. The 5-L designed reactor is well applied NMS as photocatalysts for sunlight/visible-light-driven photocatalytic disinfection for various bacteria, including Gram-negative and Gram-positive bacteria.

4. Conclusions

A 5-L reactor was designed to photocatalytically inactivate *E. coli* K-12 by NMS under different conditions. Excellent photocatalytic disinfection performance of NMS was achieved even after 5 cycles without any washing or treatment. Good stability and little deactivation of NMS showed by EES study and indicate the NMS has excellent application prospect for photocatalytic bacterial inactivation. Different bacteria, including three Gram-positive bacteria, also showed good disinfection rates by the photocatalyst of NMS. To our knowledge, this is the first study on photocatalytic inactivation of various types of bacteria by NMS in a large size reactor conducted under different conditions (at night, and in cloudy and sunny days).

Acknowledgements

The study was supported by a grant from ITSP Tier 3 Scheme (ITS/237/13) of Innovation and Technology Commission by the Hong Kong SAR Government.

References

Bhatt, V., Gohil, K., 2013. Ion exchange synthesis and thermal characteristics of some [N^{+}_{4444}] based ionic liquids. Thermochim. Acta. 556, 23–29.

Brame, J., Long, M., Li, Q., Alvarez, P., 2015. Inhibitory effect of natural organic matter or other background constituents on photocatalytic advanced oxidation processes: mechanistic model development and validation. Water Res. 84, 362–371.

Chen, Y., Lu, A., Li, Y., Zhang, L., Yip, H.Y., Zhao, H., An, T., Wong, P.K., 2011. Naturally occurring sphalerite as a novel cost-effective photocatalyst for bacterial disinfection under visible light. Environ. Sci. Technol. 45, 5689–5695.

Chen, Y., Ng, T.W., Lu, A., Li, Y., Yip, H.Y., An, T., Li, G., Zhao, H., Gao, M., Wong, P.K., 2013. Comparative study of visible-light-driven photocatalytic inactivation of two different wastewater bacteria by natural sphalerite. Chem. Eng. J. 234, 43–48.

Chen, W., Qian, C., Liu, X., Yu, H., 2014. Two-dimensional correlation spectroscopic analysis on the interaction between humic acids and TiO_2 nanoparticles. Environ. Sci. Technol. 48, 11119–11126.

Cho, M., Chung, H., Choi, W., Yoon, J., 2004. Linear correlation between inactivation of *E. coli* and OH radical concentration in TiO_2 photocatalytic disinfection. Water Res. 38, 1069–1077.

Cho, M., Cates, E., Kim, J., 2011. Inactivation and surface interactions of MS-2 bacteriophage in a TiO_2 photoelectrocatalytic reactor. Water Res. 45, 2104–2110.

Choi, W., Hoffmann, M.R., 1995. Photoreductive mechanism of CCl_4 degradation on TiO_2 particles and effects of electron donors. Environ. Sci. Technol. 29, 1646–1654.

Duan, E., Guo, B., Zhang, M., Guan, Y., Sun, H., Han, J., 2011. Efficient capture of SO_2 by a binary mixture of caprolactam tetrabutyl ammonium bromide ionic liquid and water. J. Hazard. Mater. 194, 48–52.

Elzinga, E., Huang, J., Chorover, J., Kretzschmar, R., 2012. ATR-FTIR spectroscopy study of the influence of pH and contact time on the adhesion of *Shewanella putrefaciens* bacterial cells to the surface of hematite. Environ. Sci. Technol. 46, 12848–12855.

Gamalski, A., Tersoff, J., Kodambaka, S., Zakharov, D., Ross, F., Stach, E., 2015. The role of surface passivation in controlling Ge nanowire faceting. Nano Lett. 15, 8211–8216.

Guo, W., Xu, C., Wang, X., Wang, S., Pan, C., Lin, C., Wang, Z., 2012. Rectangular bunched rutile TiO_2 nanorod arrays grown on carbon fiber for dye-sensitized solar cells. J. Am. Chem. Soc. 134, 4437–4441.

Kiwi, J., Nadtochenko, V., 2005. Evidence for the mechanism of photocatalytic degradation of the bacterial wall membrane at the TiO_2 interface by ATR-FTIR and laser kinetic spectroscopy. Langmuir 21, 4631–4641.

Li, Q., Mahendra, S., Lyon, D., Brunet, L., Liga, M., Li, D., Alvarez, P., 2008. Antimicrobial nanomaterials for water disinfection and microbial control: potential applications and implications. Water Res. 42, 4591–4602.

Mignardi, S., Corami, A., Ferrini, V., 2012. Evaluation of the effectiveness of phosphate treatment for the remediation of mine waste soils contaminated with Cd, Cu, Pb, and Zn. Chemosphere 86, 354–360.

Nakayama, A., Yano, Y., Kobayashi, S., Ishikawa, M., Sakai, K., 1996. Comparison of pressure resistances of spores of six *Bacillus* strains with their heat resistances. Appl. Environ. Microbiol. 62, 3897–3900.

Ng, T.W., Zhang, L., Liu, J., Huang, G., Wang, W., Wong, P.K., 2016. Visible-light-driven photocatalytic inactivation of *Escherichia coli* by magnetic Fe_2O_3-AgBr. Water Res. 90, 111–118.

Rodríguez-Chueca, J., Ormad, M.P., Mosteo, R., Ovelleiro, J.L., 2015. Kinetic modeling of *Escherichia coli* and *Enterococcus sp.* inactivation in wastewater treatment by photo-Fenton and H_2O_2/UV–vis processes. Chem. Eng. J. 138, 730–740.

Wang, W., Yu, Y., An, T., Li, G., Yip, H., Yu, J., Wong, P., 2012. Visible-light-driven photocatalytic inactivation of *E. coli* K-12 by bismuth vanadate nanotubes: bactericidal performance and mechanism. Environ. Sci. Technol. 46, 4599–4606.

Wiebke, A., Stefanie, H., Sonja, J., Manfred, N., Jürgen, M., 2012. Resistance phenotypes mediated by aminoacyl-phosphatidylglycerol synthases. J. Bacteriol. 194, 1401–1416.

Xia, D., Ng, T.W., An, T., Li, G., Li, Y., Yip, H.Y., Zhao, H., Lu, A., Wong, P.K., 2013. A recyclable mineral catalyst for visible-light-driven photocatalytic inactivation of bacteria: natural magnetic sphalerite. Environ. Sci. Technol. 47, 11166–11173.

Xia, D., Yan, L., Huang, G., Fong, C.C., An, T., Li, G., Yip, H., Zhao, H., Lu, A., Wong, P.K., 2015. Visible-light-driven inactivation of *Escherichia coli* K-12 over thermal treated natural pyrrhotite. Appl. Catal. B Environ. 176–177, 749–756.

Xin, J., Tang, F., Zheng, X., Shao, H., Kolditz, O., Lu, X., 2016. Distinct kinetics and mechanisms of mZVI particles aging in saline and fresh groundwater: H_2 evolution and surface passivation. Water Res. 100, 80–87.

Yamashita, Y., Jaffé, R., 2008. Characterizing the interactions between trace metals and dissolved organic matter using excitation-emission matrix and parallel factor analysis. Environ. Sci. Technol. 42 (19), 7374–7379.

Yang, X., Qin, J., Jiang, Y., Chen, K., Yan, X., Zhang, D., Li, R., Tang, H., 2015. Fabrication of P25/Ag3PO4/graphene oxide heterostructures for enhanced solar photocatalytic degradation of organic pollutant sand bacteria. Appl. Catal. B Environ. 166–167, 231–240.

Yu, H., Chen, W., Wang, X., Xu, Y., Yu, J., 2016. Enhanced photocatalytic activity and photoinduced stability of Ag-based photocatalysts: the synergistic action of amorphous-Ti (IV) and Fe (III) cocatalysts. Appl. Catal. B Environ. 187, 163–170.